

The SOPHIE search for northern extrasolar planets[★]

II. A multi-planet system around HD 9446

G. Hébrard¹, X. Bonfils², D. Ségransan³, C. Moutou⁴, X. Delfosse², F. Bouchy^{1,5}, I. Boisse¹, L. Arnold⁵, M. Desort², R. F. Díaz¹, A. Eggenberger², D. Ehrenreich², T. Forveille², A.-M. Lagrange², C. Lovis³, F. Pepe³, C. Perrier², F. Pont⁶, D. Queloz³, N. C. Santos^{3,7}, S. Udry³, A. Vidal-Madjar¹

¹ Institut d'Astrophysique de Paris, UMR7095 CNRS, Université Pierre & Marie Curie, 98bis boulevard Arago, 75014 Paris, France

² Université J. Fourier (Grenoble 1)/CNRS, Laboratoire d'Astrophysique de Grenoble (LAOG, UMR5571), France

³ Observatoire de Genève, Université de Genève, 51 Chemin des Maillettes, 1290 Sauverny, Switzerland

⁴ Laboratoire d'Astrophysique de Marseille, Université de Provence, CNRS (UMR 6110), BP 8, 13376 Marseille Cedex 12, France

⁵ Observatoire de Haute-Provence, CNRS/OAMP, 04870 Saint-Michel-l'Observatoire, France

⁶ School of Physics, University of Exeter, Exeter, EX4 4QL, UK

⁷ Centro de Astrofísica, Universidade do Porto, Rua das Estrelas, 4150-762 Porto, Portugal

Received TBC; accepted TBC

ABSTRACT

We report the discovery of a planetary system around HD 9446, performed from radial velocity measurements secured with the spectrograph *SOPHIE* at the 193-cm telescope of the Haute-Provence Observatory during more than two years. At least two planets orbit this G5V, active star: HD 9446b has a minimum mass of $0.7 M_{\text{Jup}}$ and a slightly eccentric orbit with a period of 30 days, whereas HD 9446c has a minimum mass of $1.8 M_{\text{Jup}}$ and a circular orbit with a period of 193 days. As for most of the known multi-planet systems, the HD 9446-system presents a hierarchical disposition, with a massive outer planet and a lighter inner planet.

Key words. planetary systems – techniques: radial velocities – stars: individual: HD 9446

1. Introduction

Among the more than 400 exoplanets known so far, most of them have been discovered from the reflex motion they cause to their host-star, which can be detected from stellar radial velocity wobble. Thus, accurate radial velocity measurements remain a particularly efficient and powerful technic for research and characterization of exoplanetary systems. They allow the statistic of systems to be extended by completing the minimum mass-period diagram of exoplanets, in particular towards lower masses and longer periods, as the measurement accuracy improves.

Together with the advent of the new *SOPHIE* spectrograph at the 1.93-m telescope of Haute-Provence Observatory (OHP), France, the *SOPHIE* Consortium (Bouchy et al. 2009) started in late-2006 a large observational program of exoplanets search and characterization, using the radial velocity technique. In the present paper we announce the discovery of two exoplanets around HD 9446, from radial velocity measurements secured as part of the second sub-program of the *SOPHIE* Consortium. This sub-program is a giant-planet survey on a volume-limited sample around 2000 FGK stars, requiring moderate accuracy, typically in the range $5 - 10 \text{ m s}^{-1}$ (Bouchy et al. 2009). Its goal is to improve the statistics on the exoplanet parameters and their hosting stars by increasing the number of known Jupiter-mass planets, as well as offer a chance to find new transiting giant planets in front of bright stars. *SOPHIE* sub-program-2 data were already used to report the detection of several planets (Da Silva

et al. 2008, Santos et al. 2008, Bouchy et al. 2009) and to study stellar activity (Boisse et al. 2009a). This sub-program also aims at following up transiting giant exoplanets; this allowed spectroscopic transits to be observed (Loillet et al. 2008), including the detection of the two first cases of spin-orbit misalignment, namely XO-3b (Hébrard et al. 2008) then HD 80606b (Moutou et al. 2009, Pont et al. 2009), simultaneously with the discovery of the transiting nature of the planet in this last case.

The *SOPHIE* observations of HD 9446 that allow the detection of two new planets are presented in section 2. We derive and discuss the stellar and planetary properties in sections 3 and 4 respectively, and conclude in section 5.

2. Observations

We observed HD 9446 with the OHP 1.93-m telescope and *SOPHIE*, which is a cross-dispersed, environmentally stabilized echelle spectrograph dedicated to high-precision radial velocity measurements (Perruchot et al. 2008, Bouchy et al. 2009). Observations were secured in *high-resolution* mode, allowing the resolution power $\lambda/\Delta\lambda = 75000$ to be reached. The spectra were obtained in three seasons, from November 2006 to March 2009. Depending of variable atmospheric conditions, the exposure times ranged between 3 and 18 minutes and signal-to-noise ratios per pixel at 550 nm between 32 and 94, with typical values of 5.5 minutes and 55, respectively. Exposure time and signal-to-noise ratio were slightly greater during the first season of observation. Three exposures performed through too cloudy conditions were excluded from the final dataset, that includes 79 spectra. The total exposure time is about 7 hours.

[★] Based on observations collected with the *SOPHIE* spectrograph on the 1.93-m telescope at Observatoire de Haute-Provence (CNRS), France, by the *SOPHIE* Consortium (program 07A.PNP.CON.S).

The spectrograph is fed by two optical fibers, the first one being used for starlight. During the first season the second *SOPHIE* entrance fiber was fed by a thorium lamp for simultaneous wavelength calibration. Thereafter we estimated that wavelength calibration performed with a ~ 2 -hour frequency each night (allowing interpolation for the time of the exposure) was sufficient, and that the instrument was stable enough to avoid simultaneous calibration for this moderate-accuracy program. So for the second and third seasons, no simultaneous thorium calibration were performed, avoiding pollution of the first-entrance spectrum by the calibration light. The second entrance fiber was instead put on the sky; this allowed us to check that none of the spectra were significantly affected by sky background pollution, especially due to moonlight.

We used the *SOPHIE* pipeline (Bouchy et al. 2009) to extract the spectra from the detector images, cross-correlate them with a G2-type numerical mask, then fit the cross-correlation functions (CCFs) by Gaussians to get the radial velocities (Baranne et al. 1996, Pepe et al. 2002). Each spectrum produces a clear CCF, with a $8.47 \pm 0.05 \text{ km s}^{-1}$ full width at half maximum and a contrast representing $38.0 \pm 0.8\%$ of the continuum. Only the 33 first spectral orders of the 39 available ones were used for the cross correlation; this allows the full dataset to be reduced with the same procedure, as the last red orders of the HD 9446 spectra obtained during the first season were polluted by argon spectral lines of the simultaneous wavelength-calibration.

The derived radial velocities are reported in Table 1. The accuracies are between 5.4 and 9.7 m s^{-1} , typically around 6.5 m s^{-1} . This includes photon noise (typically $\sim 3.5 \text{ m s}^{-1}$), wavelength calibration ($\sim 3 \text{ m s}^{-1}$), and guiding errors ($\sim 4 \text{ m s}^{-1}$) that produce motions of the input image within the fiber (Boisse et al. 2009b). These computed uncertainties do not include any “jitter” due to stellar activity (see below).

Table 1. Radial velocities of HD 9446 measured with *SOPHIE* (full table available electronically).

| BJD | RV | $\pm 1 \sigma$ |
|------------|------------------------|------------------------|
| -2 400 000 | (km s^{-1}) | (km s^{-1}) |
| 54043.4849 | 21.7152 | 0.0063 |
| 54045.4850 | 21.7451 | 0.0055 |
| 54047.4598 | 21.7747 | 0.0056 |
| 54048.5033 | 21.7969 | 0.0054 |
| ... | ... | ... |
| ... | ... | ... |
| 54889.2599 | 21.7201 | 0.0073 |
| 54890.2628 | 21.7409 | 0.0064 |
| 54893.2986 | 21.7222 | 0.0090 |
| 54894.2961 | 21.7074 | 0.0097 |

3. Stellar properties of HD 9446

We used the 50 *SOPHIE* spectra secured without simultaneous thorium exposure to obtain an averaged spectrum, and we managed a spectral analysis from it. Table 2 summarizes the stellar parameters. According to the SIMBAD database, HD 9446 (HIP 7245, BD+28 253) is a $V = 8.35$, high proper-motion G5V star. Its Hipparcos parallax ($\pi = 19.92 \pm 1.06 \text{ mas}$) implies a distance of $53 \pm 3 \text{ pc}$. The Hipparcos color is $B - V = 0.680 \pm 0.015$ (Perryman et al. 1997).

From spectral analysis of the *SOPHIE* data using the method presented in Santos et al. (2004), we derived the temperature

Table 2. Adopted stellar parameters for HD 9446.

| Parameters | Values |
|-------------------------------------|-------------------|
| m_v | 8.35 |
| Spectral type | G5V |
| $B - V$ | 0.680 ± 0.015 |
| Parallax [mas] | 19.92 ± 1.06 |
| Distance [pc] | 53 ± 3 |
| $v \sin i_*$ [km s^{-1}] | 4 ± 1 |
| $\log R'_{\text{HK}}$ | -4.5 ± 0.1 |
| [Fe/H] | 0.09 ± 0.05 |
| T_{eff} [K] | 5793 ± 22 |
| $\log g$ [cgs] | 4.53 ± 0.16 |
| Mass [M_{\odot}] | 1.0 ± 0.1 |
| Radius [R_{\odot}] | 1.0 |
| Luminosity [L_{\odot}] | 1.1 |

$T_{\text{eff}} = 5793 \pm 22 \text{ K}$, the gravity $\log g = 4.53 \pm 0.16$, $[\text{Fe}/\text{H}] = +0.09 \pm 0.05$, and $M_* = 1.0 \pm 0.1 M_{\odot}$. The 10% uncertainty on the stellar mass is an estimation, systematic effects being difficult to quantify (Fernandes & Santos 2004). We derive a projected rotational velocity $v \sin i_* = 4 \pm 1 \text{ km s}^{-1}$ from the parameters of the CCF using the calibration of Boisse et al. (in preparation), which is similar to that presented by Santos et al. (2002). We also obtained $[\text{Fe}/\text{H}] = +0.12 \pm 0.10$ from the CCF, which agrees with, but is less accurate than the metallicity obtained from our spectral analysis.

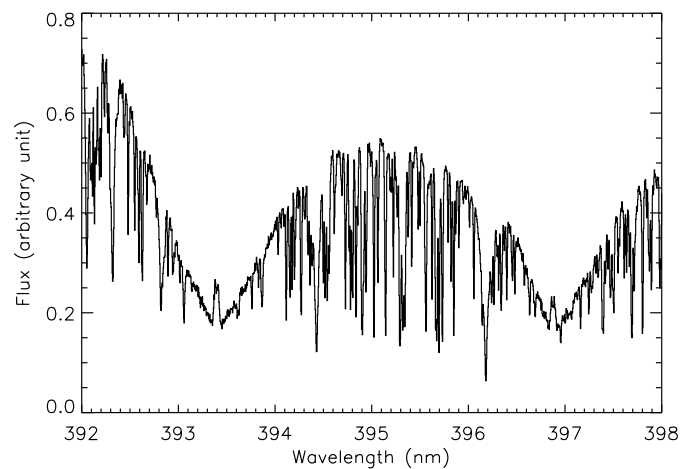


Fig. 1. H and K Ca II lines of HD 9446 on the averaged *SOPHIE* spectra. Chromospheric emissions are detected, yielding a $\log R'_{\text{HK}} = -4.5 \pm 0.1$.

The cores of the large Ca II absorption lines of HD 9446 show small emissions (Fig. 1), which are the signature of an active chromosphere. Such stellar activity would imply a significant “jitter” on the stellar radial velocity measurement. The level of the Ca II emission corresponds to $\log R'_{\text{HK}} = -4.5$ with a ± 0.1 dispersion according to the *SOPHIE* calibration (Boisse et al. in preparation). For a G-type star with this level of activity, Santos et al. (2000) predict a dispersion of the order of 10 to 20 m s^{-1} for the stellar jitter. According to Noyes et al. (1984) and Mamajek & Hillenbrand (2008), this level of activity implies a stellar rotation period $P_{\text{rot}} \approx 10$ days. This agrees with

our $v \sin i_*$ measurement, which translates into $P_{\text{Rot}} < 17$ days (Bouchy et al. 2005), depending on the unknown inclination i_* of the stellar rotation axes.

4. A planetary system around HD 9446

The *SOPHIE* radial velocities of HD 9446 are plotted in Fig. 2. Spanning more than two years, they show clear variations of the order of 200 m s^{-1} , implying a dispersion $\sigma_{\text{RV}} = 58 \text{ m s}^{-1}$; this is well over the expected stellar jitter due to chromospheric activity (10 to 20 m s^{-1} , see above). In addition, the bisectors of the CCF are stable (Fig. 3, upper panel), showing dispersion of the order of $\sigma_{\text{BIS}} = 20 \text{ m s}^{-1}$, well below that of the radial velocities. An anticorrelation between the bisector and the radial velocity is usually the signature of radial velocity variations induced by stellar activity (see, e.g., Queloz et al. 2001, Boisse et al. 2009a). The bisectors are flat by comparison with the radial velocities, which suggests that the radial velocity variations are mainly due to Doppler shifts of the stellar lines rather than stellar profile variations. This leads to conclude that reflex motion due to companion(s) are the likely cause of the stellar radial velocity variations.

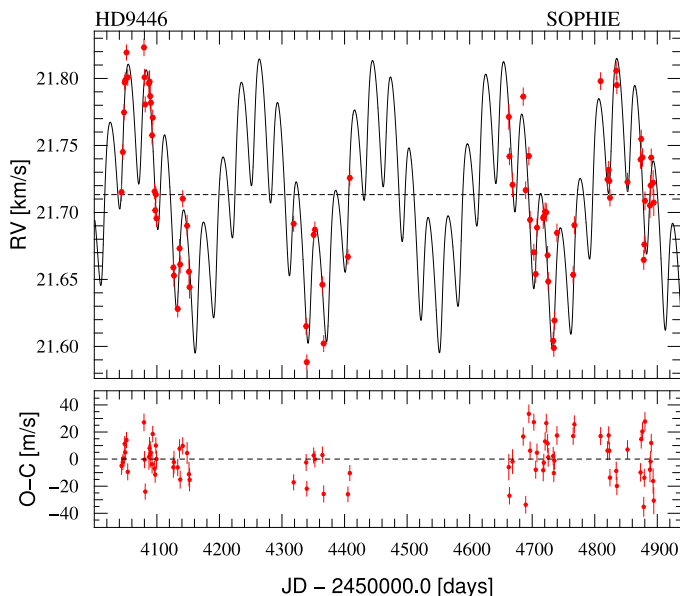


Fig. 2. *Top:* Radial velocity *SOPHIE* measurements of HD 9446 as a function of time, and Keplerian fit with two planets. The orbital parameters corresponding to this fit are reported in Table 3. *Bottom:* Residuals of the fit with $1\text{-}\sigma$ error bars.

These facts were known in late 2007, after two seasons of *SOPHIE* observations of HD 9446. A search of Keplerian fits then produced a solution with two Jupiter-like planets, on orbits of 30 and 190 days of period, with low eccentricities. This solution was thereafter confirmed by the third season of observation; together with the “flat” bisectors, this provides a strong support to the two-planet interpretation of the radial velocity variations.

Figs. 2 and 4 show the final fit of the 851-day span *SOPHIE* radial velocities of HD 9446. This Keplerian model includes two planets without mutual interactions, which are negligible in this case (see Sect. 5). All the parameters are free to vary during the fit. The derived orbital parameters are reported in Table 3, to-

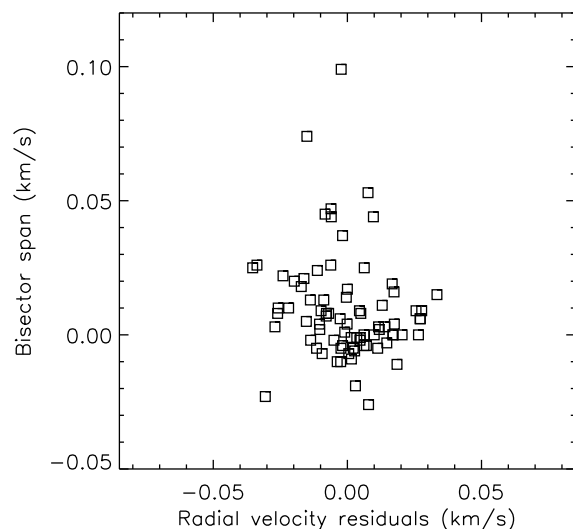
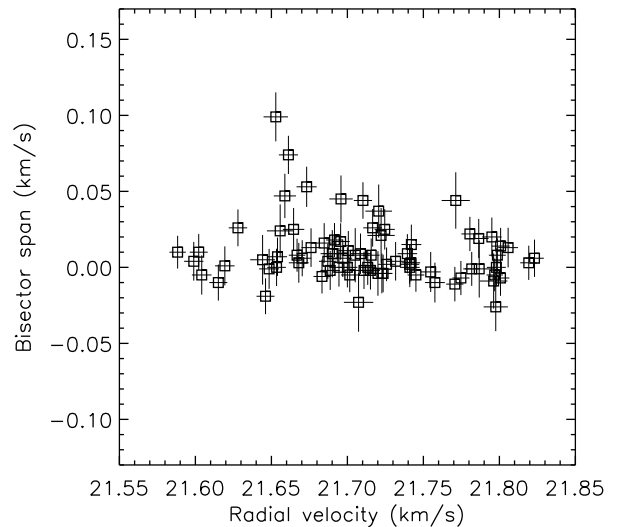


Fig. 3. Bisector span as a function of the radial velocity (top) and the radial velocity residuals after the 2-planet fit (bottom). For clarity, error bars are not plotted in the bottom panel. The ranges have the same extents in the x - and y -axes on both panels.

gether with error bars, which were computed from χ^2 variations and Monte Carlo experiments.

The inner planet, HD 9446b, produces radial velocity variations with a semi-amplitude $K = 46.6 \pm 3.0 \text{ m s}^{-1}$, corresponding to a planet with a minimum mass $M_{\text{p}} \sin i = 0.70 \pm 0.06 M_{\text{Jup}}$ (assuming $M_* = 1.0 \pm 0.1 M_{\odot}$ for the host star). Its orbit has a period of 30.052 ± 0.027 days, and is significantly non-circular ($e = 0.20 \pm 0.06$). This period is longer than the stellar rotation period, as determined above from the $\log R'_{\text{HK}}$ and the $v \sin i_*$. A P_{rot} -value of 30 days would correspond to $v \sin i_* < 2 \text{ km s}^{-1}$, which is incompatible with our data. The outer planet, HD 9446c, yields a semi-amplitude $K = 63.9 \pm 4.3 \text{ m s}^{-1}$, corresponding to a planet with a projected mass $M_{\text{p}} \sin i = 1.82 \pm 0.17 M_{\text{Jup}}$. The orbital period is 192.9 ± 0.9 days. This is about half a Earth-year, which made difficult a good phase coverage for the obser-

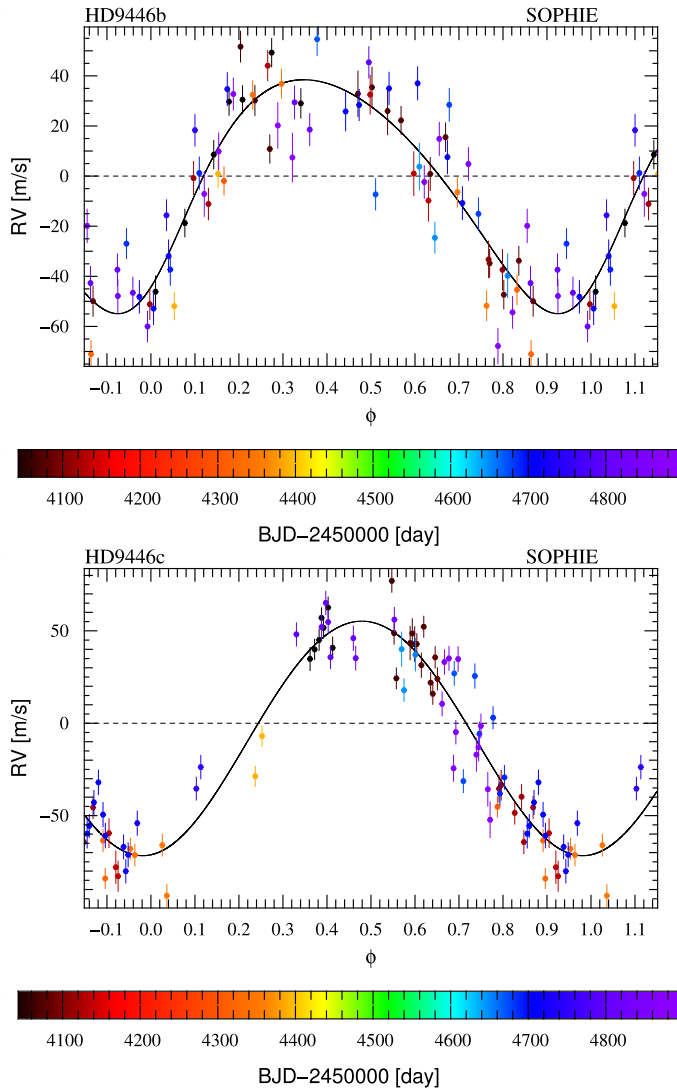


Fig. 4. Phase-folded radial velocity curves for HD 9446b ($P = 30$ d, top) and HD 9446c ($P = 193$ d, bottom) after removing the effect of the other planet. The *SOPHIE* radial velocity measurements are presented with $1\text{-}\sigma$ error bars, and the Keplerian fits are the solid lines. Orbital parameters corresponding to the fits are reported in Table 3. The colors indicate the measurement dates.

vations. As seen in the lower panel of Fig. 4, the rise of the radial velocity due to HD 9446c lacks of measurements, for orbital phases between 0.0 and 0.3. This implies significant uncertainties on the shape of the orbit. Circularity can not be excluded ($e = 0.06 \pm 0.06$); furthermore, if the orbit actually is eccentric, there are nearly no constraints with the present dataset on the orientation of the ellipse with respect to the line of sight. The resulting error bars on the longitude ω of the periastron and on the time T_0 at periastron are thus large; there are however correlated, and the timing of a possible transit for this planet is better constrained than T_0 in Table 3. Our estimations of $v \sin i_*$ and P_{rot} allow the constraint $i_* > 30^\circ$ to be put. So, if we assume a spin-orbit alignment for the HD 9446-system, $i_* = i$ and $\sin i > 0.5$; this implies projected masses that translate into actual masses clearly in the planetary range.

Table 3. Fitted orbits and planetary parameters for the HD 9446 system, with $1\text{-}\sigma$ error bars.

| Parameters | HD 9446b | HD 9446c |
|---------------------------------------------|----------------------------|----------------------------|
| P [days] | 30.052 ± 0.027 | 192.9 ± 0.9 |
| e | 0.20 ± 0.06 | 0.06 ± 0.06 |
| ω [$^\circ$] | -145 ± 30 | -260 ± 130 |
| K [m s^{-1}] | 46.6 ± 3.0 | 63.9 ± 4.3 |
| T_0 (periastron) [BJD] | $2\,454\,854.4 \pm 2.0$ | $2\,454\,510 \pm 70$ |
| $M_{\text{p}} \sin i$ [M_{Jup}] | $0.70 \pm 0.06^\ddagger$ | $1.82 \pm 0.17^\ddagger$ |
| a [AU] | $0.189 \pm 0.006^\ddagger$ | $0.654 \pm 0.022^\ddagger$ |
| V_r [km s^{-1}] | 21.715 ± 0.005 | |
| N | 79 | |
| reduced χ^2 | 2.6 | |
| $\sigma_{\text{O-C}}$ [m s^{-1}] | 15.1 | |
| Typical RV accuracy [m s^{-1}] | 6.5 | |
| span [days] | 851 | |

‡ : using $M_* = 1.0 \pm 0.1 M_\odot$

The reduced χ^2 of the Keplerian fit is 2.6, and the standard deviation of the residuals is $\sigma_{\text{O-C}} = 15.1 \text{ m s}^{-1}$. This is better than the 58-m s^{-1} dispersion of the original radial velocities, but this remains higher than the 6.5-m s^{-1} typical error bars on the individual measurements, suggesting an additional noise of $\sim 13.5 \text{ m s}^{-1}$. Such dispersion is precisely in the range of the 10 to 20 m s^{-1} expected jitter for a G-type star with this level of activity (Sect. 3). Stellar activity is thus likely to be the main cause of the remaining dispersion, as well as the $\sim 20\text{-m s}^{-1}$ dispersion of the bisectors. The residuals of the fits do not show significant anticorrelation with the bisectors (Fig. 3, lower panel), as it could be expected in such cases (see, e.g., Melo et al. 2007, Boisse et al. 2009a); this is however at the limit of detection according to the error bars. A few bisectors values are larger than the other ones. They could be due to a particularly active phase of the star, as they are localized in a short time interval (between late January and early February 2007). Excluding these outliers from the analysis does not significantly change the results. Finally, as it can be seen on lower panel of Fig. 2, the residuals are significantly less scattered during the first season than during the third one. This can be mainly explained by the higher signal-to-noise ratio reached with longer exposure times during the first season, as well as the simultaneous thorium calibration secured for the first measurements.

Figure 5 shows Lomb-Scargle periodograms of the radial velocity measurements of HD 9446 in four different cases: without any planet removed, with one or the other planet removed, and with both planets removed. A similar study was performed in the case of BD $-08^\circ 2823$, another star with two detected planets (Hébrard et al. 2009). In the upper panel of Fig. 5 that presents the periodogram of the raw radial velocity measurements of HD 9446, periodic signals at ~ 30 days and ~ 195 days are clearly detected with peaks at those periods, corresponding to the two planets reported above, with the same amplitudes. The peak at ~ 1 day corresponds to the aliases of all the detected signals, as the sampling is biased towards “one point per night”. A fourth, weaker peak is detected at ~ 13.3 days. A Keplerian fit of this signal would provide a semi-amplitude $K \simeq 11 \text{ m s}^{-1}$, corresponding to a projected mass of 40 Earth masses. We do not conclude, however, that we detect a third, low-mass planet within the current data.

Indeed, firstly this 13.3-day period is near the stellar rotation period (~ 10 days, Sect. 3), so it could be at least partially due to stellar rotation. However, no significant peaks are detected at this period (nor at 30 days or 193 days) on the bisectors peri-

odograms. We interpret this 13.3-d signal as being more likely due to aliases. In order to validate this, we constructed a fake radial velocity dataset with the same time sampling as our actual data, and that includes only the Keplerian model of the two planets found above. The periodogram of this fake dataset is almost identical as the one plotted in the upper panel Fig. 5: it includes of course the two peaks corresponding to the periods of the two planets, but also the peak at 13.3 days.

In addition to the one-day peak, the window function of our data shows a peak at ~ 14.3 days, indicating that this interval is favored in our time sampling. The 13.3-d signal could thus be mainly due to the 14.3-day alias of the 192.9-day signal ($1/13.3 \approx 1/14.3 + 1/192.9$). On the second panel of Fig. 5 is plotted the periodogram of the residuals after subtraction of a fit including the 30-day-period planet only. The peak at 193 days is visible, as well as these aliases at 1, 13.3, and 15.4 days ($1/15.4 \approx 1/14.3 - 1/192.9$). In the same manner, the third panel of Fig. 5 shows the periodogram of the residuals after a fit including the 193-day-period planet only. The peak at 193 days is no longer visible, and neither are the three aliases seen on the upper panel. This time the peak at 30 days is visible, together with these two aliases due to the 1-day favored sampling, at 0.97 and 1.03 day. The bottom panel of Fig. 5 shows the periodogram of the residuals after subtraction of the Keplerian fit including HD 9446b and HD 9446c. There are no remaining strong peaks on this periodogram; even the 1-day alias disappeared, showing that most of the periodic signals have been removed from the data. The remaining peaks are below 10 m/s amplitude, showing that the main part of the detected periodical signals in our data are due to the two planets. The remaining signal in the residuals are at the limit of detection according to our accuracy. As in addition the stellar rotation period is close to an alias of the signal of HD 9446c, this makes tough any characterization of radial-velocity signal due to stellar activity, which is expected mainly at the stellar rotation period. As the stellar jitter on the radial velocities is of the order of 10 m s^{-1} , this effect on the derived parameters of the two detected planets is negligible.

The residuals of the measurements secured during the second observational season are preferentially negative (Fig. 2, lower panel). This may suggest a possible additional component, with an orbital period of the same order or larger than the time span of our dataset (2.3 years). Such an additional planet could not be established with the available data. For a ~ 2 -yr period, the projected mass of such a hypothetical planet should be lower than one Jupiter mass. On the other hand on short periods, a hot-Jupiter is excluded in this system, the accuracy of our dataset being good enough to detect it if there were any. The data allow planets with masses larger than $0.3 M_{\text{Jup}}$ and orbital periods shorter than 10 days to be excluded in the HD 9446 system.

5. Discussion

The data we presented allow us to conclude there is a planetary system around HD 9446, with at least two Jupiter-like planets, on 30 and 193-day orbits. HD 9446b has a projected mass slightly lower than Jupiter; it is on a 0.2-eccentricity orbit, showing that tidal effects were not strong enough to circularize it. HD 9446c is at least 1.8 times more massive than Jupiter, and is on a nearly-circular orbit. The host-star of this system is slightly more metallic than the Sun, in agreement with the tendency found for stars harboring Jupiter-mass planets (see, e.g., Santos et al. 2005).

The mutual gravitational interactions between HD 9446b and HD 9446c are weak. The inner planet is stabilized on its orbit by the strong gravity of the star. Following Correia et al. (2005), a

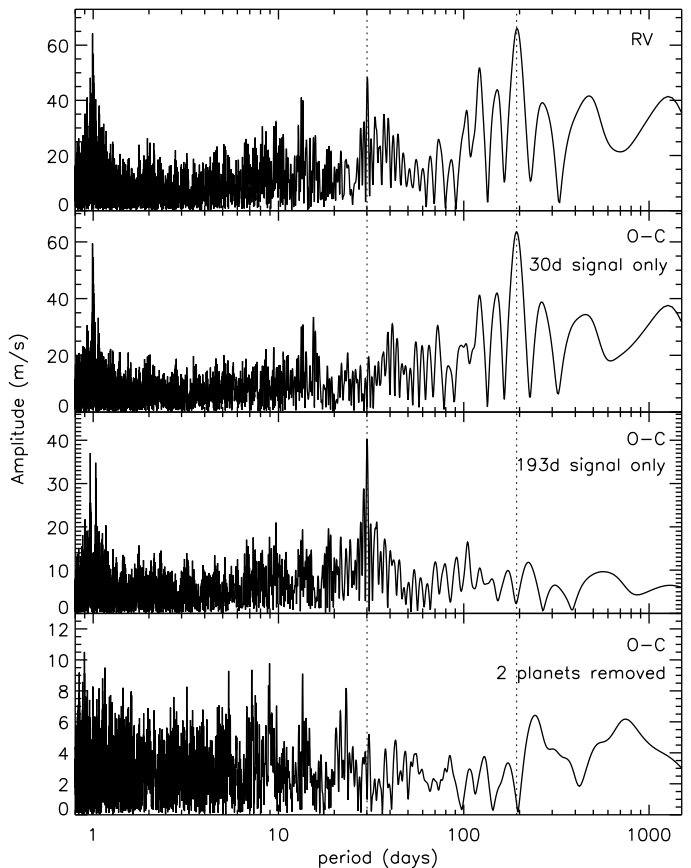


Fig. 5. Lomb-Scargle periodograms of the *SOPHIE* radial velocities. The upper panel shows the periodogram computed on the initial radial velocities, without any fit removed. The second and third panels show the periodograms computed on the residuals of the fits including HD 9446b or HD 9446c only, respectively. The bottom panel shows the periodogram after the subtraction of the 2-planet fit. The two vertical dotted lines show the periods of the two planets.

simulation of the two orbits from the current solution was run for 10^6 years, in order to estimate their evolution from mutual interactions. This shows no significant changes in the eccentricities, which remain in the ranges $[0.18 - 0.23]$ and $[0.03 - 0.075]$, for HD 9446b and HD 9446c respectively. Therefore this system is stable for 10^6 years, and it seems to be stable for longer time scales also. We estimated the order of magnitude of the potential transit timing variations due to those weak mutual interactions, if any of the planets of the system does transit. For that purpose we performed another 3-body simulation of the system, assuming the masses of the planets are equal to the minimum masses and that the orbits are coplanar. We employed the Burlisch-Stoer algorithm implemented in the Mercury6 package (Chambers 1999) and integrated the system for 2000 days -i.e. around 10 orbits of the exterior planet. We found that the interaction between the planets produces variations in the central time of transits with small amplitude, that does not exceed 0.4 second for any of the two bodies.

No photometric search for transits have been managed for HD 9446; depending on the unknown inclination i of the orbit, the transit probability for HD 9446b and HD 9446c are about 2% and 1%, respectively. There are more than 200 exoplanets detected from radial velocity surveys with orbital periods longer than 50 days, so with transit probabilities of the level of the percent. Only one is known to transit, namely HD 80606b (Moutou et al. 2009). It is likely that at least one or two more of these known long-period exoplanets are actually transiting as seen from the Earth. Their search is challenging, as the times of the possible transits are not known accurately, especially a few years after the securement of the radial velocity data.

Among the more than 400 exoplanets discovered so far, almost 25% are located in the ~ 40 known multiple-planet systems. Most of them have been detected from radial velocity measurements. Additional planetary companions around HD 9446 can not be detected with the available data besides the two planets reported, but they are of course possible, as multiple-planet systems are common. For example HD 155358 (Cochran et al. 2007) has a Jupiter-mass planet on an orbit similar to HD 9446c, and another planet with a 530-day orbital period, or HD 69830 (Lovis et al. 2006) have two Neptune-mass planets on orbits similar to those of the two detected planets of HD 9446, and a third one on a 8.7-day orbit. More data are needed, and the monitoring of HD 9446 should thus be maintained. As low-mass planets are preferentially found in multiple planetary systems (see, e.g., McArthur et al. 2004, Pepe et al. 2007, Mayor et al. 2009), HD 9446 should be considered for high-precision radial-velocity programs, despite its activity level.

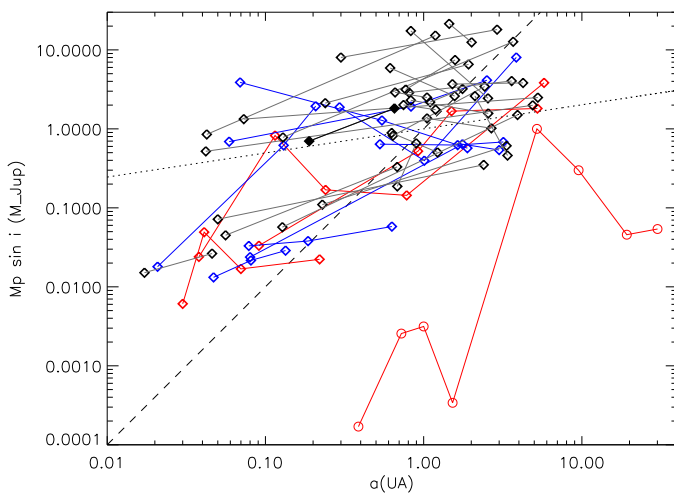


Fig. 6. Semi-major axes as a function of the projected masses for planets in multi-planet systems. 38 known extrasolar systems are plotted, with the planets of a given system that are linked by a solid line. The HD 9446-system is shown with filled diamonds. The fitted relation is plotted in dotted line (mass proportional to $a^{0.3}$); the dashed line show the a^2 relation. The 8 planets of the Solar System are also plotted for comparison (circles). Systems with two, three and more planets are in black, blue and red, respectively.

The HD 9446 system presents a hierarchical disposition, with the inner planet being the less massive one and the outer planet being the more massive. Fig. 6 displays the mass –

semi-major axis relation for known multi-planetary systems. The data are taken from the compilation of the Extrasolar Planets Encyclopedia¹. Most of the known multi-planetary systems show such hierarchical disposition, as roughly the Solar System. The fitted relation between those two parameters provides a planet mass proportional to $a^{0.3}$ ($\propto a^{1.5}$ for the Solar System). The plot suggests the slope could be deeper for systems including low-mass planets. A positive slope could be due to a higher migration efficiency for low-mass planets, and/or to the fact that giant planets are preferentially formed at larger distances of their host stars than low-mass planets. However, observational biases are important here, as low-mass planets are easier to detected at short orbital periods from radial velocity variations. The semi-amplitude of the reflex motion of a star due to a planetary companion is proportional to $\sqrt{a} \times M_p \sin i$, so one could expect a a^2 -dependance in Fig. 6. As the averaged slope is lower, this could suggest there is actually no strong dependance on average between those two parameters for multi-planet systems.

Fig. 6 also shows that only a few multi-planetary systems include close-in giant planets. This agrees with Wright et al. (2009), who reported that single-planet systems show a pileup at 3-day period and a jump at $a \approx 1$ AU, while multi-planet systems show a more uniform distribution. Still, the close-in planets in known multi-planet system are mainly low-mass planets. Hot Jupiters appear to be sparse in multi-planet systems, showing here again a distribution which is different from single-planet systems. Only five hot-Jupiters are known to be in planetary systems, namely HIP 14810b, ups And b, HAT-P-13b, HD 187123b, and HD 217107b. Single- and multi-planet systems thus appear to have significant differences in some of their properties. Such differences may provide clues allowing a better understanding of the formation and evolution of those systems. Improving the statistic of extra-solar planets should be continued, in particular in multi-planet systems and with radial velocity surveys.

Acknowledgements. We thank A. C. M. Correia for helps and discussions, as well as all the staff of Haute-Provence Observatory for their support at the 1.93-m telescope and on *SOPHIE*. We thank the “Programme National de Planétologie” (PNP) of CNRS/INSU, the Swiss National Science Foundation, and the French National Research Agency (ANR-08-JCJC-0102-01 and ANR-NT05-4-44463) for their support to our planet-search programs. NCS would like to thank the support by the European Research Council/European Community under the FP7 through a Starting Grant, as well from Fundação para a Ciência e a Tecnologia (FCT), Portugal, through a Ciência 2007 contract funded by FCT/MCTES (Portugal) and POPH/FSE (EC), and in the form of grants reference PTDC/CTE-AST/098528/2008 and PTDC/CTE-AST/098604/2008 from FCT/MCTES.

References

- Baranne, A., Queloz, D., Mayor, M., et al. 1994, *A&AS*, 119, 373
- Boisse, I., Moutou, C., Vidal-Madjar, A., et al. 2009a, *A&A*, 495, 959
- Boisse, I., Bouchy, F., Chazelas, B., Perruchot, S., Pepe, F., Lovis, C., Hébrard, G. 2009b, *New technologies for probing the diversity of brown dwarfs and exoplanets*, EPJ Web of Conferences, in press
- Bouchy, F., Pont, F., Melo, C., Santos, N. C., Mayor, M., Queloz, D., Udry, S., 2005, *A&A*, 431, 1105
- Bouchy, F., Hébrard, G., Udry, S., et al. 2009, *A&A*, 505, 853
- Chambers, J.E. 1999, *MNRAS*, 304, 793
- Cochran, W. D., Endl, M., Wittenmyer, R. A., Bean, J. L. 2007, *ApJ*, 665, 1407
- Correia, A. C. M., Udry, S., Mayor, M., Laskar, J., Naef, D., Pepe, F., Queloz, D., Santos, N. C. 2005, *A&A*, 440, 751
- Da Silva, R., Udry, S., Bouchy, F., et al. 2008, *A&A*, 473, 323
- Fernandes, J., Santos, N. C. 2004, *A&A*, 427, 607
- Hébrard, G., Bouchy, F., Pont, F., et al. 2008, *A&A*, 481, 52
- Hébrard, G., Udry, S., Lo Curto, G., et al. 2009, *A&A*, in press [arXiv:0912.3202]

¹ <http://exoplanet.eu>

- Loeillet, B., Shporer, A., Bouchy, F., et al. 2008, *A&A*, 481, 529
- Lovis, C., Mayor, M., Pepe, F., et al. 2006, *Nature*, 441, 305
- McArthur, B., Endl, M., Cochran W., et al. 2004, *ApJ*, 614, L81
- Mamajek, E. E., & Hillenbrand, L. A. 2008, *ApJ*, 687, 1264
- Mayor, M., Udry, S., Lovis, C., et al. 2009, *A&A*, 493, 639
- Melo, C., Santos, N. C., Gieren, W., et al. 2007, *A&A*, 467, 721
- Moutou, C., Hébrard, G., Bouchy, F., et al. 2009, *A&A*, 498, L5
- Noyes, R. W., Hartmann, L. W., Baliunas, S. L., Duncan, D. K., Vaughan, A. H. 1984, *ApJ*, 279, 763
- Pepe, F., Mayor, M., Galland, F., et al. 2002, *A&A*, 388, 632
- Pepe, F., Correia, A. C. M., Mayor, M., et al. 2007, *A&A*, 462, 776
- Perruchot, S., Kohler, D., Bouchy, F., et al., 2008, in *Ground-based and Airborne Instrumentation for Astronomy II*, Edited by McLean, I.S., Casali, M.M., Proceedings of the SPIE, vol. 7014, 70140J
- Perryman, M. A. C., Lindegren, L., Kovalevsky, J., et al. 1997, *A&A*, 323, L49
- Pont, F., Hébrard, G., Irwin, J. M., et al. 2009, *A&A*, 509, 695
- Queloz, D., Henry, G. W., Sivan, J. P., et al. 2001, *A&A*, 379, 279
- Santos, N. C., Mayor, M., Naef, D., et al. 2000, *A&A*, 361, 265
- Santos, N. C., Mayor, M., Naef, D., et al. 2002, *A&A*, 392, 215
- Santos, N. C., Israelian, G., Mayor, M. 2004, *A&A*, 415, 1153
- Santos, N. C., Israelian, G., Mayor, M., et al. 2005, *A&A*, 437, 1127
- Santos, N. C., Udry, S., Bouchy, F., et al. 2008, *A&A*, 487, 369
- Wright, J. T., Upadhyay, S., Marcy, G. W., Fischer, D. A., Ford, E. B., Johnson, J. A. 2009, *ApJ*, 693, 1084